Energy Proceedings
Vol 26, 2022
ISSN 2004-2965

On the Conversion of Diesel Engines to Dedicated Ammonia: Lean, Stoichiometric or Rich Operation[#]

Jinlong Liu[1], Christopher J. Ulishney[1], Cosmin E. Dumitrescu[1*]

1 Department of Mechanical and Aerospace Engineering, West Virginia University, Morgantown, WV 26506, USA

ABSTRACT

Ammonia, a carbon-free fuel, can make an important contribution towards the decarbonization of on- and off-road internal combustion (IC) engines. However, the research on the ammonia use in IC engines is still in initial stages. The goal of this study was to investigate the effect of the equivalence ratio on an ammonia-dedicated engine performance. To observe how the equivalence ratio of the air-ammonia mixture affects in-cylinder flame speed and the reaction pathway of pollutant formation (therefore, how it affects engine efficiency and emissions), a multi-dimensional computational fluid dynamics simulation of a single-cylinder diesel engine converted to dedicated ammonia spark ignition operation was built. The numerical results suggested that stoichiometric operation was better than lean operation for this engine. In detail, lean operation reduced the combustion efficiency and increased engine-out NO_X and ammonia emissions, therefore potentially discarding the known thermal efficiency benefit of lean operation in IC engines. In addition, a rich equivalence ratio drastically reduced combustion and thermal efficiency, and increased fuel consumption rates and unburned engine-out ammonia emissions. Finally, while stoichiometric operation produced the best overall performance in terms of efficiency and emissions, attention must be paid to N_2O and unburned NH_3 engine-out emissions.

Keywords: internal combustion engine, zero-carbon ammonia fuel, spark ignition, 3D CFD simulation, air-fuel ratio, engine combustion and emission formation

NONMENCLATURE

Abbreviations	
3D	Three Dimensional
ATDC/BTDC	After/BeforeTop Dead Center
CA	Crank Angle
CA*x*	CA related to *x*% Energy Release
CFD	Computational Fluid Dynamics
CI	Compression Ignition
DOC	Duration of Combustion
H/H_2	Hydrogen Radical/Molecule
HRR	Heat Release Rate
IMEP	Indicated Mean Effective Pressure
ISFC	Indicated Specific Fuel Consumption
LPP	Peak Pressure Location
N	Engine Speed or Nitrogen
NH_3	Ammonia
NO/NO_2	Nitrogen Monoxide/Dioxide
NO_X	Nitrogen Oxides
N_2O	Nitrous Oxide
OH	Hydroxyl Radical
PCP	Peak Cylinder Pressure
SI	Spark Ignition
ST	Spark Timing
Symbols	
ϕ	Equivalence Ratio
η_{comb}	Combustion Efficiency
η_{th}	Thermal Efficiency
P_{intake}	Intake Pressure
T_{intake}	Intake Temperature

1. INTRODUCTION

The use of carbon-free fuels for internal combustion (IC) engines is both a great opportunity and challenge in the global trend of decarbonizing on- and off-road internal combustion (IC) engines [1]. Ammonia, a carbon-free fuel, is a strong contender inside the pool of possible alternative fuels because of its mature production technology and easy storage and transportation [2]. Accordingly, the use of ammonia in IC engines can improve the traditional energy structure and achieve the target in reducing carbon emissions [3].

Ammonia (NH_3) is a hydrogen-rich carrier containing 17.6% by mass hydrogen. A distinct advantage of using ammonia as an IC engine fuel is that it is carbon-free; hence, its combustion does not emit carbon dioxide or soot [1]. However, despite its attractive characteristics, there is limited research on the ammonia use in IC engines [4]. Consequently, a systematic study of the co-optimization of ammonia fuel properties with the IC engine design is warranted [5]. For example, a better understanding of the effect of the air-fuel ratio in dedicated ammonia engines can suggest a combination of advanced combustion technology and aftertreatment

that would meet increasingly stringent emissions regulations. Since the pollutant conversion efficiency using a three-way catalyst can exceed 95% if the equivalence ratio is around unity [6], gasoline engines always operate on a stoichiometric air-fuel mixture. But it is known that lean operation can reduce thermal nitrogen oxides (NO_X) and improve engine efficiency [6]. However, it may require a more advanced and expensive aftertreatment. As a result, the choice of air-fuel ratio during the engine design must consider both the aftertreatment cost and efficiency and the fuel characteristics. Fig. 1 shows a sketch of the ammonia oxidation pathway [7]. Complete ammonia combustion produces only nitrogen and water, but also increases the pathway of fuel NO_X generation. In other words, it is possible that lean engine operation may not significantly reduce NO_X emissions [8]. Since NH_3 also has a denitrification effect, ammonia rich combustion can reduce the NO_X concentration in the exhaust, at the expense of a higher fuel consumption rate. Another important issue is the very slow laminar flame speed of ammonia (just one-sixth of that of gasoline [9]), which peaks at slightly fuel-rich operation, and lean operation further reduces it. Therefore, it is needed to determine if a dedicated ammonia engine should operate lean, stoichiometric, or rich. Once known, a combination of selective catalytic reduction and ammonia slip catalyst could be used to reduce NO_X and unburned ammonia. Therefore, finding the optimal equivalence ratio is a prerequisite towards the development of dedicated ammonia engines. As a result, this study used three dimensional (3D) computational fluid dynamics (CFD) simulations to assess the effect of the equivalence ratio on engine performance and emissions formation. The objective was to provide additional knowledge about the lean, stoichiometric, or rich operation in dedicated ammonia engines.

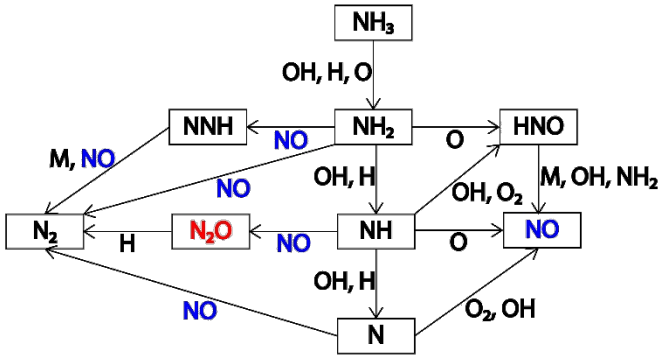

Fig. 1 Ammonia oxidation pathway

2. MATERIALS AND METHODS

The engine used for modeling in-cylinder ammonia combustion is a single-cylinder, four-stroke, heavy-duty ported fuel injection spark ignition (SI) engine, converted from a direct injection compression ignition (CI) engine, with a bore of 130.2 mm, a stroke of 150 mm, a compression ratio of 13.3, and a flat-head and bowl-in-piston combustion chamber. For gaseous fuel operation, a spark plug, installed in place of the diesel injector, initiated and controlled the combustion process, and a low-pressure gas injector, added upstream of the intake valve, delivered the fuel. It may be preferable to use converted compression ignition engines for pure ammonia operation because their high compression ratios and good flow motions would accelerate the flame propagation of a fuel with a slow laminar flame speed such as ammonia [10]. More details about the engine setup can be found in ref. [11].

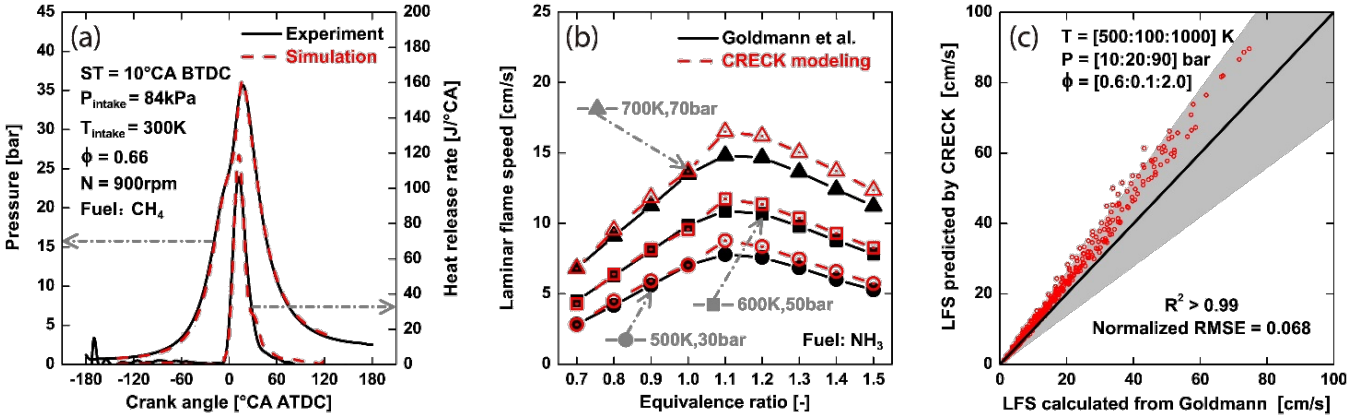

Fig. 2 3D CFD model validation: (a) comparison of 3D CFD model predicted and experimental pressure trace and heat release rate for the engine fueled with methane, (b) effect of equivalence ratio on laminar flame speed of ammonia at high pressure and high temperature conditions, using Goldmann's regression relationships or the CRECK chemical mechanism, and (c) comparison of ammonia laminar flame speed under typical in-cylinder conditions, using Goldmann's regression relationships or the CRECK chemical mechanism

A Reynolds Averaged Navier-Stokes (RANS) numerical simulation was operated between intake valve closing and exhaust valve opening, assuming a homogeneous mixture of air and ammonia. In-cylinder turbulent compressible flow was simulated with an RNG k-ε model specifically designed for engines [12]. The level-set approach (G-equation) predicted the fully developed turbulent flame propagation and the discrete particle ignition kernel flame (DPIK) model predicted the kernel generation with a Lagrangian approach [12]. The global Cartesian grid size was 2.5 mm, and the grid refinement strategy was applied to the region around the spark plug and to the layers near the walls. The 3D CFD model was validated with experimental data from natural gas operations, with details discussed in ref. [11]. The good agreement between the model predictions and experimentally measured pressure trace and heat release rate shown in Fig. 2a demonstrates the perfect calibration of the predictive combustion model. In terms of the chemistry, the CRECK detailed mechanism consisting of 31 species and 203 reactions [13] characterized ammonia combustion. High temperature and pressure laminar flame speed predictions using the above chemistry were compared to those derived by Goldmann using regression methods [14], as those are considered the standard.

Fig. 2b shows that the CRECK mechanism predicted well the effect of equivalence ratio, pressure, and temperature on ammonia's laminar flame speed. In addition, Fig. 2c shows a comparison between the CRECK laminar flame speed predictions and Goldmann's regression relationships for temperatures between 500 K and 1000 K in 100-K increments, pressures between 10 bar and 90 bar in 20-bar increments, and equivalence ratios between 0.6 and 2.0 in 0.1 increments. Although the CRECK chemical mechanism predicted a slightly larger laminar flame speed, the differences were acceptable, as ~91.5% of the predictions were within 30% of the variance (defined as a qualifying threshold [15]), the coefficient of determination (R^2) was greater than 0.9, and the normalized root-mean-square error (RMSE) was less than 0.1 [16]. Overall, the calibrated combustion model together with the appropriate ammonia chemistry was deemed reasonable to describe the activities inside the dedicated ammonia internal combustion engine [17].

3. RESULTS AND DISCUSSION

The predictive capability of the 3D CFD model was used to investigate the effect of the equivalence ratio on engine performance. Fig. 3 shows the engine power output, thermal efficiency, and emissions, for lean, stoichiometric, or rich ammonia-air mixtures. The results show that the engine achieved good combustion for an equivalence ratio as low as 0.8, at 15° CA BTDC spark timing (ST) and 900 rpm engine speed, despite the low laminar flame speed of ammonia. This was due to the high compression ratio and the "fast-burn" feature of the bowl-in-piston chamber, as mentioned in the *Introduction* section. As expected, the cylinder pressure rose with increasing equivalence ratio, from lean to stoichiometric operation, as the fuel energy per cycle increased and the flame propagation process was faster. Cylinder pressure barely changed when the equivalence ratio varied from 1 to 1.2, but as shown in Fig. 3b, the pressure rise rate increased. However, the maximum pressure rise rate remained below 10 bar/° CA, indicating that the flame propagation process dominated the combustion (i.e., no knocking). While the peak cylinder pressure (PCP) shown in Fig. 3c peaked for $\phi = 1.1$ at the spark timing and engine speed studied here, it was less sensitive to the equivalence ratio when ϕ was between 1.0 and 1.2, which echoed the almost unchanged cylinder pressure shown in Fig. 3a. However, Fig. 3d shows that the bulk temperature decreased significantly for an air-fuel mixture richer than stoichiometry, probably due to differences in adiabatic flame temperature. As expected, leaner operation significantly reduced the bulk temperature due to the reduced chemical energy of the fuel-air mixture. Fig. 3e shows the effect of equivalence ratio on the apparent heat release rate (HRR), calculated with a single-zone heat-release model. The leaner mixture operation showed a smaller and retarded second HRR peak, due to a slower flame propagation process. The laminar flame speed of ammonia was similar when the equivalence ratio was between 1.0 and 1.2, which contributed to the similar HRR curves. The most important information in Fig. 3e was that the bulk combustion finished almost at ~40°CA ATDC, regardless of the equivalence ratio. Fig. 3f shows that the engine indicated mean effective pressure (IMEP) reached a maximum when operated at stoichiometry. A leaner operation reduced the IMEP due to less chemical energy per cycle, while a richer operation lowered the power output because of incomplete combustion. The peak pressure location (LPP) and the heat release centroid (CA50) are two combustion phasing metrics used to determine optimal conditions. As indicated in ref. [18], optimum LPP and CA50 are usually found between ~9°CA and ~16°CA ATDC and between ~5°CA and ~11°CA ATDC, respectively. The LPP shown in Figure 3g indicated that the 15°CA BTDC ST was within the optimal ST range for all equivalence ratios investigated here, while the CA50 data shown in Figure 3h suggested that the optimal ST for leaner operation should be more advanced than those used for gasoline or natural gas

operation. Lean operation usually improves the thermal efficiency (η_{th}), which explains the peak thermal efficiency at ϕ=0.9 in Fig. 3i. Further leaning the mixture to ϕ=0.8 reduced the engine efficiency, due to a retarded combustion phasing relative to the optimum value. Indicated specific fuel consumption (ISFC) was the inverse of engine efficiency. As a result, the minimum ISFC occurred at ϕ=0.9. It is worth noting that the value of ISFC was ~500 g/kWh, much larger than that for gasoline or natural gas engines. This was due to ammonia having a smaller lower heating value. In addition, ϕ>1.0 significantly increased ISFC compared to stoichiometric operation, suggesting that the rich operation may not be an optimal. Figs 3k and 3i present the effect of equivalence ratio on the ignition lag (defined as the crank angle interval between ST and CA10) and duration of combustion (DOC; the difference between CA90 and CA10), respectively. Lean operation prolonged the ignition lag and duration of combustion, as the slower flame speed delayed and extended the burning event.

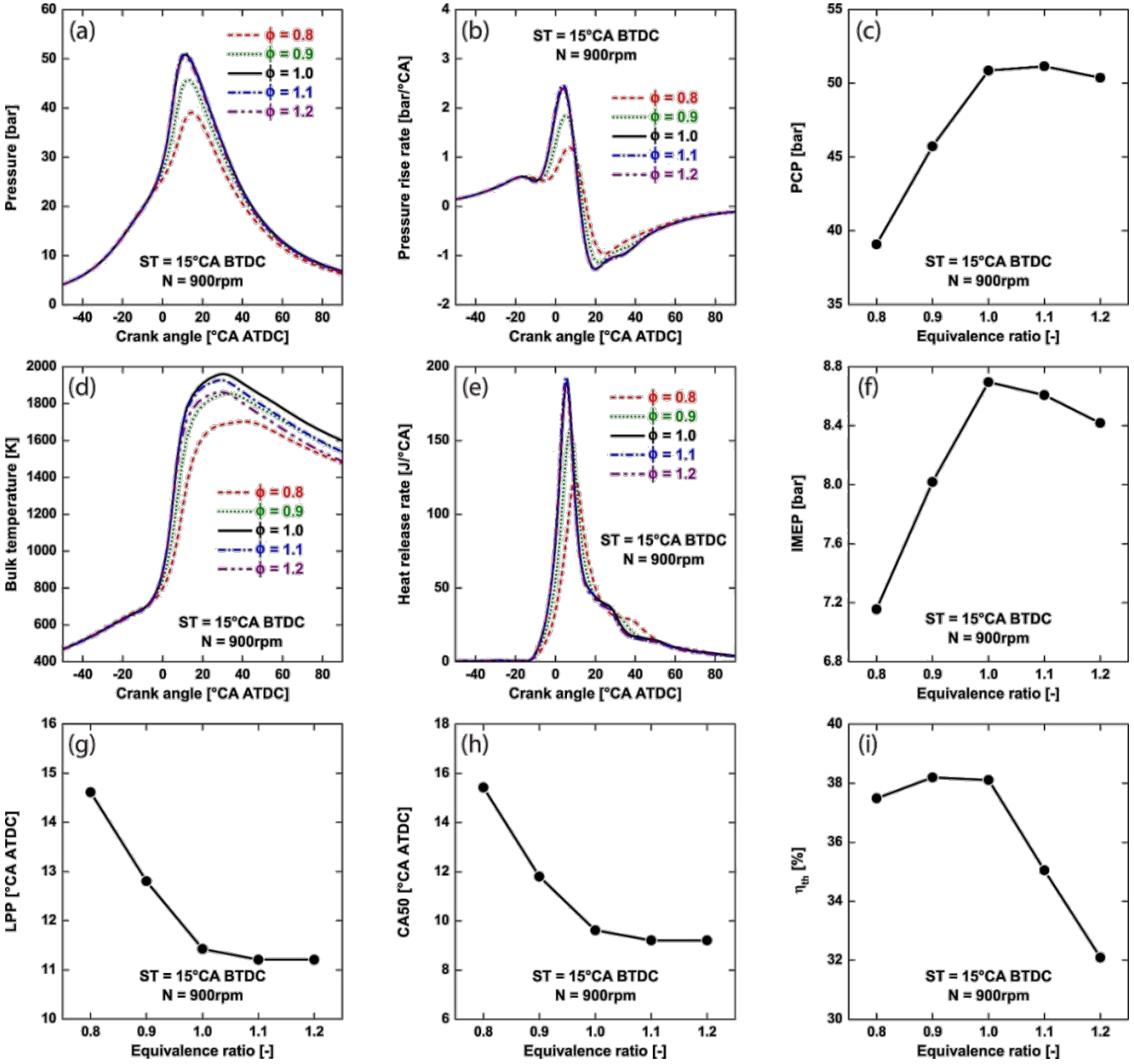

Fig. 3 Performance of the ammonia engine operating at lean, stoichiometric and rich conditions

Figs. 3m, 3n and 3o show the NO_X, NO_2, and N_2O emissions, respectively. In contrast to a hydrocarbon-fueled engine, lean operation with ammonia greatly increased NO_X emissions. The phenomenon was attributed to the dominant fuel NO_X formation mechanism. The ~3-fold increase in the indicated specific NO_X for ϕ<1 compared to the stoichiometric operation suggested that the lean operation may not be optimal. Fuel-rich operation greatly reduced NO_X, due to the lack of oxygen to form NO_X and because of the de-NO_X effect

of ammonia. The small NO_2 and N_2O emissions shown in Figs. 3n and 3o indicate the NO dominance in NO_X (>98%), similar with what is seen for gasoline (or natural gas) SI operation. Engine emissions of N_2O and NO_2 increased with decreasing ϕ. While the NO_2 was almost zero under stoichiometric operation, N_2O was non-negligible when considering that N_2O is a very strong greenhouse gas (i.e., it is 300x more potent than CO_2). As shown in Fig. 3p, the ammonia emissions from the stoichiometric operation were minimal. Unburned fuel trapped in engine crevices during combustion was believed to be the cause of emitted ammonia in the exhaust. The level of unburned ammonia increased for lean operation, probably due to the reduced chemical reactivity of ammonia and the low temperature environment, both of which were detrimental to late oxidation of the crevice-trapped ammonia. The increase in unburned ammonia emissions for rich operation was mainly due to the higher concentration of ammonia trapped in the crevice. As for the hydrogen emissions, Fig. 3q shows that the indicated specific H_2 increased with ϕ and underwent a sharp increase from stoichiometric to rich operation. This was because excess ammonia was decomposed into hydrogen. The sharp decrease in combustion efficiency (η_{comb}) and the not so high growth of unburned ammonia for rich operation suggested that H_2 emissions accounted for a large part of the combustion incompleteness. This phenomenon resulted in a lower ammonia emission for ϕ=1.2 than for ϕ=0.8, although η_{comb} was ~17% lower. It is also important to note that the peak combustion efficiency was ~95% at ϕ=1.0.

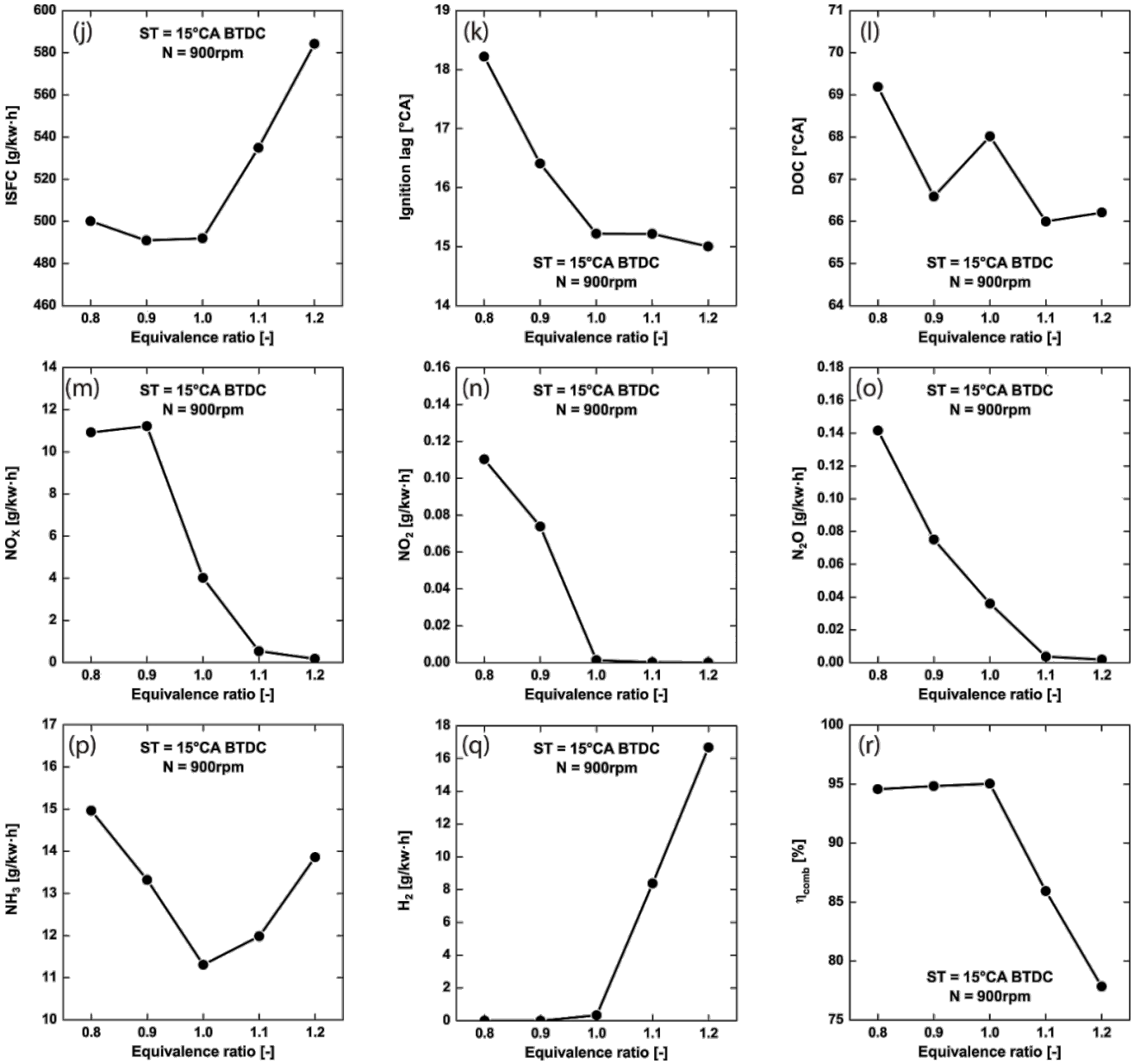

Fig. 3 (continued)

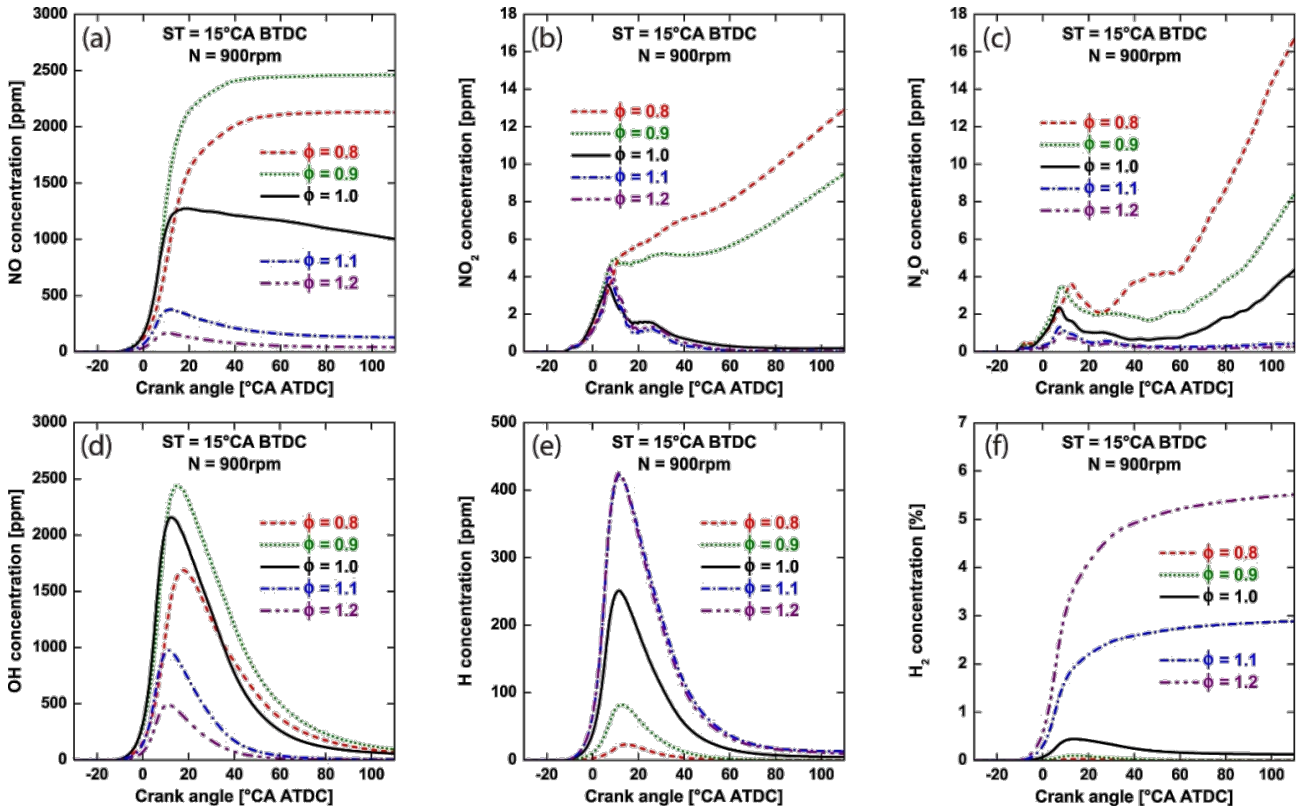

Fig. 4 Formation process of selected species in the chamber of the ammonia engine operating at lean, stoichiometric and rich conditions

A benefit of engine 3D CFD combustion modeling is the ability to predict the formation and consumption of chemical species of interest. Fig. 4 shows the effect of equivalence ratios on the dynamic change of spatially averaged concentration of selected species (NO, NO_2, and N_2O, OH, H, and H_2), which can help to further understand in-cylinder ammonia combustion. Fig. 4a shows that NO concentration peaked at ~10°CA ATDC for ϕ=1.0, 1.1 and 1.2, before being consumed in subsequent reactions, therefore reducing NO emissions in the exhaust. In contrast, lean operation had a rapid NO formation process from spark timing to ~40°CA ATDC and remained almost constant until exhaust valve opened, hence a high level of NO_X in the exhaust. For stoichiometric and rich operation, Fig. 4b shows that NO_2 concentration peaked at ~9°CA ATDC and then underwent a decreasing process, which led to an almost zero concentration of NO_2 at exhaust valve opening. By comparison, the NO_2 concentration for lean operation continued to increase after ~9°CA ATDC until exhaust valve opened but at a smaller rate, which resulted in a NO_2 concentration of the same order of magnitude as the N_2O concentration in the exhaust. The effect of equivalence ratio on the N_2O formation and consumption history shown in Fig. 4c suggested that N_2O formation rate was smaller for rich operation once the combustion started, which led to a low peak at ~9°CA ATDC, and then experienced a continuous N_2O depletion process, eventually achieving equilibrium during late oxidation. However, N_2O increased again after the first peak for lean and stoichiometric operations, but at different crank angles, hence different N_2O levels in the exhaust. The ammonia oxidation pathway shown in Fig. 1 indicates that the formation and consumption of NO_X always interact with reactive radicals such as O, OH, and H. Further, O and OH radicals have oxidizing effects and are mainly responsible for oxidizing the N-H chemical bond to form NO. Similarly, the H radical has a reducing effect, which consumes NO during combustion. As a result, the concentrations of OH and H radicals shown in in Figs. 4d and 4e can assist in the analysis of the effect of equivalence ratio on NO_X concentration. The ammonia rich operation greatly reduced the OH radicals due to the lack of oxygen, which led to larger concentrations of NH radicals to consume NO. By contrast, lean operation resulted in a smaller percentage of H radicals but a larger OH concentration, which increased the possibility of breaking the N-H bond to form NO. The abundant H radicals produced by the rich ammonia combustion also inhibited the dissociation of H_2, which resulted in the continuous formation of hydrogen in the cylinder, as shown in Fig. 4f. For stoichiometric operation, the hydrogen concentration peaked at ~10°CA ATDC, while H_2 was barely found in lean operation.

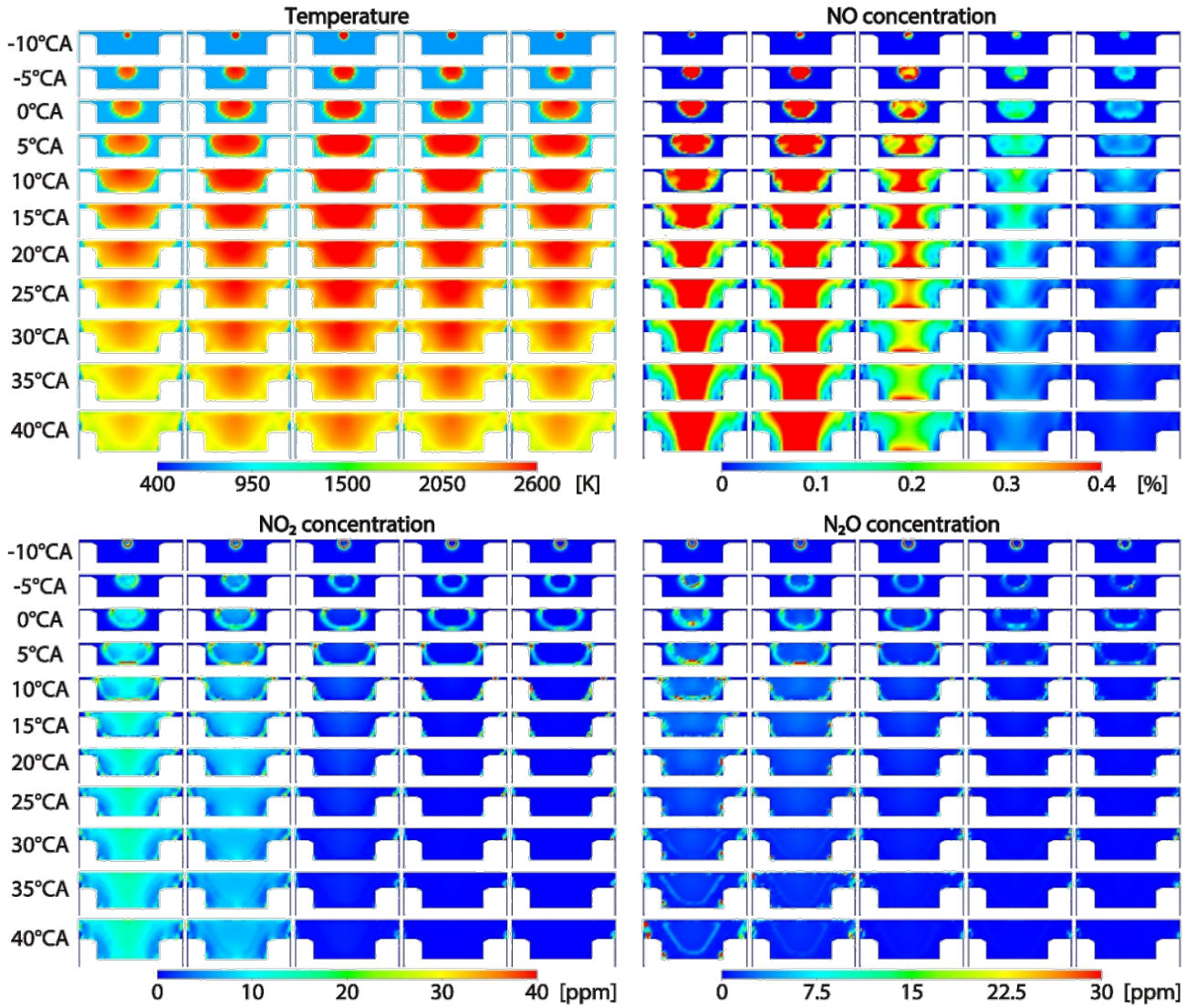

Fig. 5 Distribution of temperature and concentration of selected species in the chamber during combustion of the ammonia engine operating at lean, stoichiometric and rich conditions

For a better understanding of the mechanisms of pollutant formation, it is also of interest to study the effect of equivalence ratio on the spatial and temporal distribution of these species inside the cylinder. Fig. 5 shows the temperature and NO_X (including NO, NO_2, and N_2O) concentration distribution in a vertical section of the cylinder. The junction between the high-temperature and low-temperature regions (i.e., burned and unburned zones) in Figure 5a is the turbulent flame location. Lean operation had a retarded flame propagation process. Moreover, stoichiometric operation resulted in a larger temperature in the burned zone, evident between 20°CA to 40°CA ATDC, consistent with the differences shown in Fig. 3d. The differences in the NO and temperature distribution in Fig. 5 again indicated the specificity of the NO formation mechanism. For traditional SI engines, the high NO concentration zone should be in the high temperature zone because thermal NO is formed by the high temperature oxidation of diatomic nitrogen in the combustion air temperature and its concentration depends on the residence time of nitrogen at that temperature [19]. The difference shown here indicated that the major source of NO came from the nitrogen-bearing ammonia fuel.

For lean operation, the NO concentration in the center of the bowl was larger despite the lower temperature near the boundary (i.e., near the cylinder head and piston top). NO was formed mainly in the central region of the bowl for stoichiometric operation, from spark to 10°CA ATDC but was consumed from 20°CA to 40°CA ATDC. Rich operation also formed NO in the burned zone, but most of it was reduced by the amino with the piston downward movement. The N_2O concentration for stoichiometric and rich operations shown in Fig. 3 indicates that it was mainly formed and consumed as an intermediate product in the flame front

region, since NO_2 was highly oxidizing at high temperatures and was easily reduced to NO during combustion. By comparison, NO_2 for lean operation was distributed throughout the combustion chamber, with same order of magnitude concentrations throughout the cylinder. N_2O was an intermediate product in the flame front region for stoichiometric and rich operations, while some N_2O was formed in the burned zone for lean operation, but then consumed to a much smaller amount than its value in the flame front zone. It is also important to mention that the OH and H radicals showed a similar concentration distribution to that of the temperature, but the results are not shown here. In detail, the lean operation had an abundant OH but very low H concentrations in the burned zone, with an opposite trend for rich operation. Moreover, the distribution of OH and H radicals affected the NO, NO_2, and N_2O distributions.

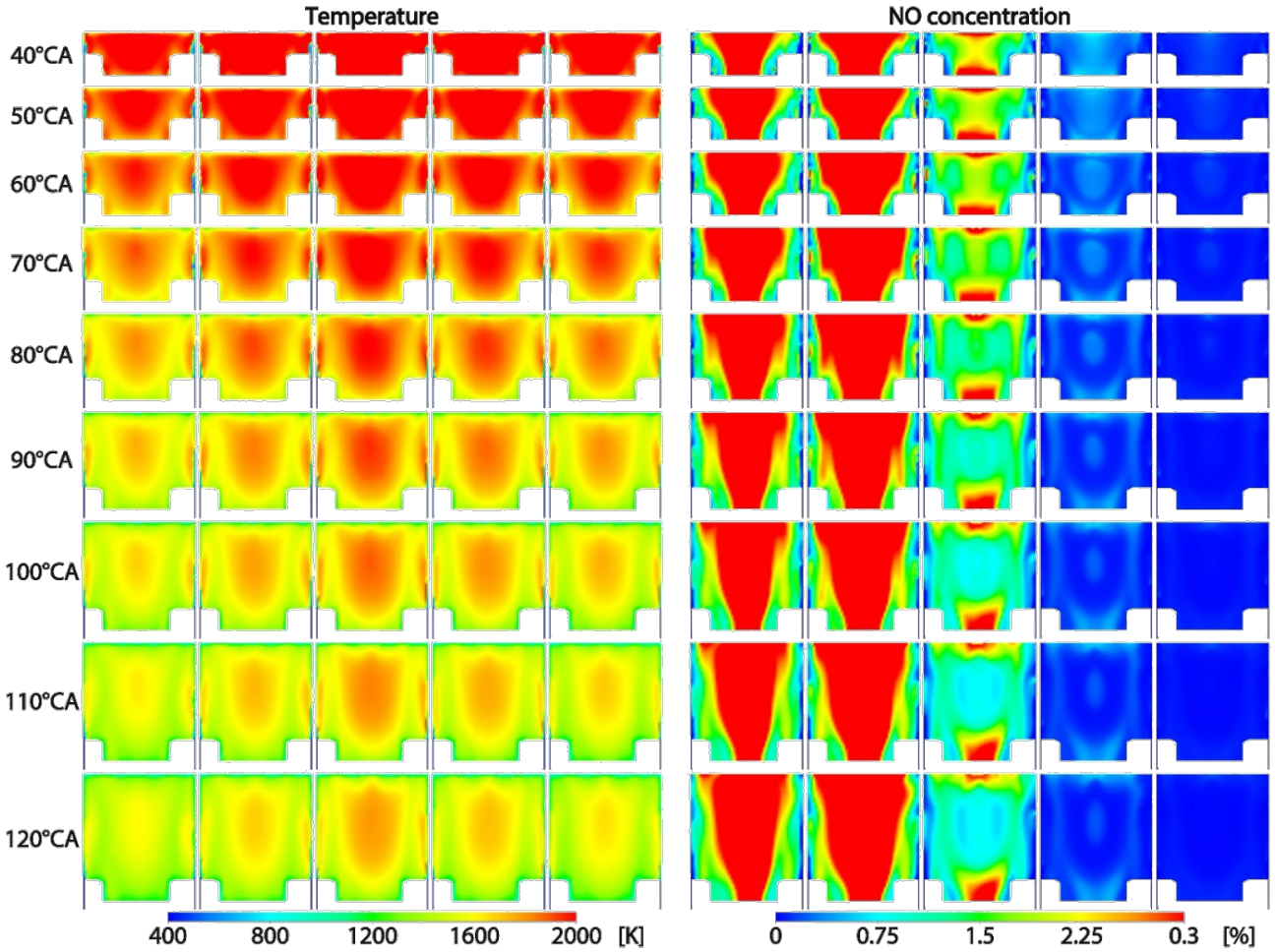

Fig. 6 Distribution of temperature and concentration of selected species in the chamber during late oxidation of the ammonia engine operating at lean, stoichiometric and rich conditions

Fig. 6 shows the same spatial distribution of the scalars in Fig. 5 for the late oxidation process, before exhaust valve opened. The temperature decreased with the piston downward movement, with the temperature for stoichiometric operation remaining the highest. Moreover, from 100°CA ATDC to 120°CA ATDC, the temperature inside the chamber entered the intermediate level, except for the central region of the bowl, for all equivalence ratios. Fig. 6 also shows that NO_2 continued to form in the burned zone during late oxidation for lean operation and had extremely high concentrations in the area near the cylinder head. However, there was almost no NO_2 left in the combustion chamber for stoichiometric and rich operations. In addition, it seems that N_2O formed during combustion was not the main source of N_2O concentration in the exhaust, since these formed N_2O were later consumed. In other words, the crevice-released ammonia during expansion experienced a low-temperature oxidation process, forming a large amount of N_2O when exhaust valve opened. A smaller ϕ operation produced more N_2O, as evidenced by the larger high-N_2O area near the liner. It is also interesting that stoichiometric operation also formed N_2O in the burned zone except the bowl center during the late expansion stroke, but in smaller concentrations

compared to the values near the crevice entrance. This was because the temperature in this region was favorable for the formation of N_2O (i.e., the intermediate temperature level mentioned before). However, N_2O was not significantly produced inside the bowl during late oxidation for lean operation, due to the lack of NH radicals that reacted with NO to form N_2O. A similar situation was seen for N_2O production for rich operation because of the lack of NO radicals to form N_2O and many H radicals available to reduce N_2O. All these results showed that the equivalence ratio has an important effect on the emission characteristics of dedicated ammonia engines.

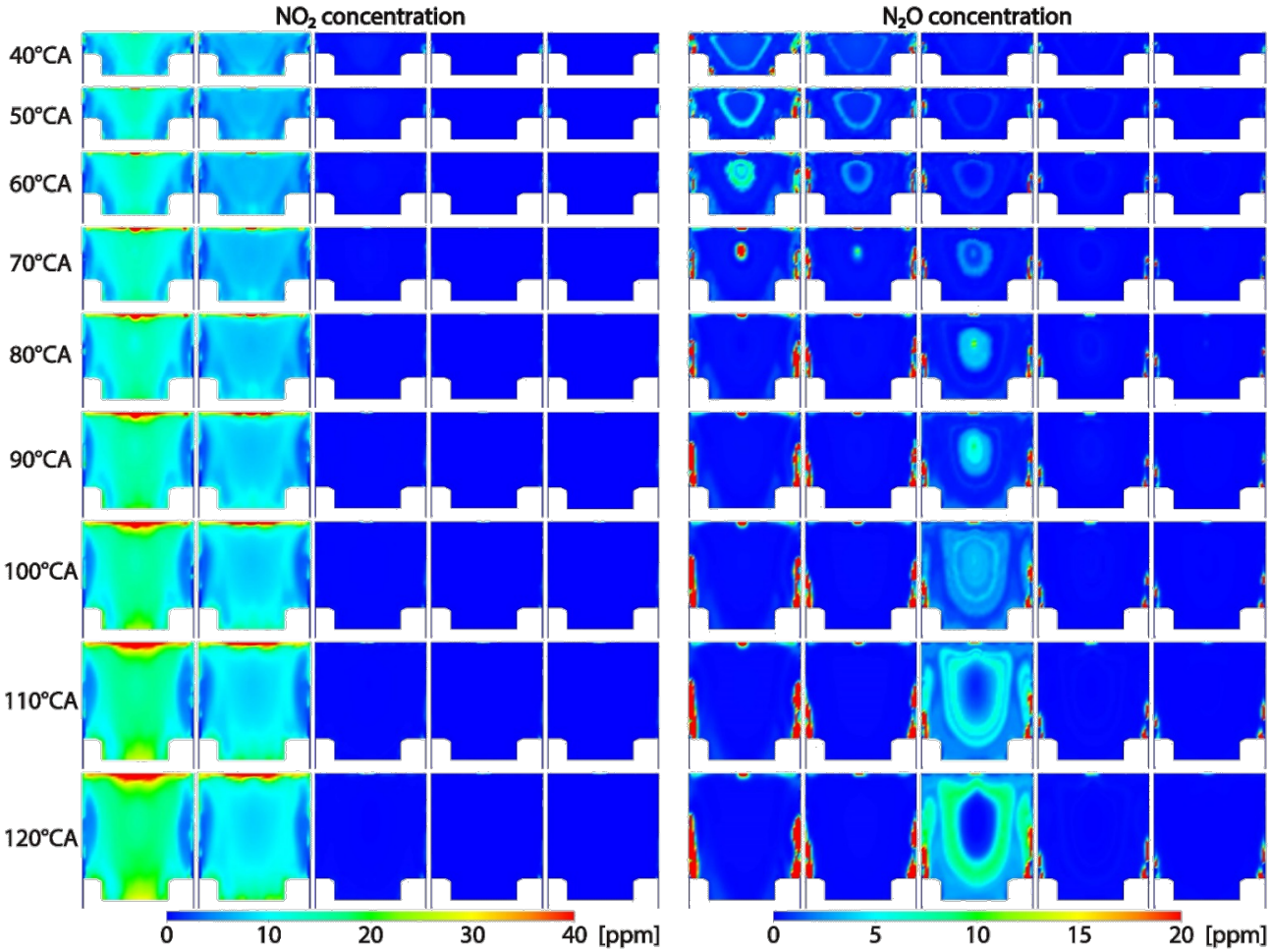

Fig. 6 (continued)

4. SUMMARY AND CONCLUSIONS

This study used a 3D CFD simulation with a detailed chemical mechanism to investigate the effect of the equivalence ratio effects on the efficiency and emissions of a diesel engine converted to pure ammonia spark ignition operation. The major findings were:

• Ammonia lean operation produced large concentrations of NO_X and NH_3 in the exhaust. The fuel NO mechanism dominated, and the abundant oxygen formed more O and OH radicals, which increased NO formation. The unburned NH_3 was mainly coming from the fuel trapped inside the crevices. In addition, N_2O and NO_2 exhaust concentrations were comparable. N_2O came mainly from the low temperature oxidation of crevice-trapped ammonia during late oxidation, while NO_2 was formed throughout the whole chamber because of the oxidation effect of the abundant OH radicals.

• Ammonia rich operation dramatically reduced the engine efficiency and increased the fuel consumption, despite extremely low NO_X emissions. This was because the formation of NO_X was prohibited by the abundant NH and H radicals. The extra ammonia was dissociated into hydrogen during combustion, which contributed to a large amount of H_2, but no sharp increase in the unburned NH_3.

• For ammonia stoichiometric operation, NO_2 was an intermediate product, which resulted in close-to-zero NO_2 emissions. Although NO was the main species of NO_X, N_2O formed from crevice trapped NH_3 also contributed a certain amount. The maximum combustion efficiency was ~95%, due to the non-

negligible unburned NH_3 and despite a near-optimal spark timing. As a result, more fundamental research is needed to co-optimize the ammonia fuel properties with the engine system design.

CONTACT INFORMATION

Cosmin E. Dumitrescu
Associate Professor
West Virginia University
P.O. Box 6106
Morgantown, WV 26506, USA
Tel.: 304-293-3330
Fax: 304-293-6689
Email: cedumitrescu@mail.wvu.edu

ACKNOWLEDGEMENT

This research was conducted at the West Virginia University (WVU) Advanced Combustion Laboratory in Morgantown, WV. The authors gratefully acknowledge WVU's Center for Alternative Fuels Engines and Emissions (CAFEE), WVU's Center for Innovation in Gas Research and Utilization (CIGRU), and the MAE department for their support and assistance.

REFERENCE

[1] Cardoso JS, Silva V, Rocha RC, Hall MJ, Costa M, Eusébio D. Ammonia as an energy vector: Current and future prospects for low-carbon fuel applications in internal combustion engines. Journal of Cleaner Production. 2021; 296: 126562.

[2] Berwal P, Kumar S, Khandelwal B. A comprehensive review on synthesis, chemical kinetics, and practical application of ammonia as future fuel for combustion. Journal of the Energy Institute. 2021; 99: 273-298.

[3] Chehade G, Dincer I. Progress in green ammonia production as potential carbon-free fuel. Fuel. 2021; 299: 120845.

[4] MacFarlane DR, Cherepanov PV, Choi J, Suryanto BH, Hodgetts RY, Bakker JM, Vallana FM, Simonov AN. A roadmap to the ammonia economy. Joule. 2020; 4(6): 1186-2105.

[5] Zamfirescu C, Dincer I. Using ammonia as a sustainable fuel. Journal of Power Sources. 2008; 185(1): 459-465.

[6] Heywood JB. Internal combustion engine fundamentals, 2nd edition. New York: McGraw-Hill; 2018.

[7] Kobayashi H, Hayakawa A, Somarathne KK, Okafor EC. Science and technology of ammonia combustion. Proceedings of the Combustion Institute. 2019; 37(1): 109-133.

[8] Shrestha KP, Seidel L, Zeuch T, Mauss F. Detailed kinetic mechanism for the oxidation of ammonia including the formation and reduction of nitrogen oxides. Energy & Fuels. 2018; 32(10): 10202-10217.

[9] Hayakawa A, Goto T, Mimoto R, Arakawa Y, Kudo T, Kobayashi H. Laminar burning velocity and Markstein length of ammonia/air premixed flames at various pressures. Fuel. 2015; 159: 98-106.

[10] Klüssmann JN, Ekknud LR, Ivarsson A, Schramm J. Ammonia application in CI engines. Special Report, A Report from the Advanced Motor Fuels Technology Collaboration Programme. 2020.

[11] Stocchi I, Liu J, Dumitrescu CE, Battistoni M, Grimaldi CN. Effect of piston crevices on the numerical simulation of a heavy-duty diesel engine retrofitted to natural-gas spark-ignition operation. Journal of energy resources technology. 2019; 141(11): 112204.

[12] ANSYS® Forte Theory. Ansys, Inc; Release 17.2.

[13] Stagni A, Cavallotti C, Arunthanayothin S, Song Y, Herbinet O, Battin-Leclerc F, Faravelli T. An experimental, theoretical, and kinetic-modeling study of the gas-phase oxidation of ammonia. Reaction Chemistry & Engineering. 2020; 5(4): 696-711.

[14] Goldmann A, Dinkelacker F. Approximation of laminar flame characteristics on premixed ammonia/hydrogen/nitrogen/air mixtures at elevated temperatures and pressures. Fuel. 2018; 224: 366-378.

[15] Chen Z. Effects of radiation absorption on spherical flame propagation and radiation-induced uncertainty in laminar flame speed measurement. Proceedings of the Combustion Institute. 2017; 36(1): 1129-1136.

[16] Mathieu O, Petersen EL. Experimental and modeling study on the high-temperature oxidation of Ammonia and related NO_X chemistry. Combustion and Flame. 2015; 162(3): 554-570.

[17] Xiao H, Valera-Medina A, Bowen PJ. Modeling combustion of ammonia/hydrogen fuel blends under gas turbine conditions. Energy & Fuels. 2017; 31(8): 8631-8642.

[18] Caton JA. Combustion phasing for maximum efficiency for conventional and high efficiency engines. Energy Conversion and Management. 2014; 77: 564-576.

[19] Bessler W, Hofmann M, Zimmermann F, Suck G, Jakobs J, Nicklitzsch S, Lee T, Wolfrum J, Schulz C. Quantitative in-cylinder NO-LIF imaging in a realistic gasoline engine with spray-guided direct injection. Proceedings of the Combustion Institute. 2005; 30: 2667-2674.